THE ASTROPHYSICAL JOURNAL, 299:616–632, 1985 December 15


# AN ANALYSIS OF THE BASEL STAR CATALOG

JOHN N. BAHCALL AND KAVAN U. RATNATUNGA
Institute for Advanced Study, Princeton, New Jersey
AND
ROLAND BUSER, R. P. FENKART, AND ANDREAS SPAENHAUER
Astronomisches Institut der Universität Basel, Switzerland
*Received 1984 October 22; accepted 1985 June 18*

## ABSTRACT

The standard Bahcall-Soneira Galaxy model is compared with the data from the 12 fields in the Basel star catalog that are at Galactic latitudes above 20° and have $E(B-V) < 0.1$ mag. Good agreement is found between the calculated and observed color distributions, as well as star counts, for all the fields. The globular cluster feature that is observed in the luminosity function of globular clusters near $M_V = +1$ to $+4$ mag is also present in the spheroid field stars. It is possible to assign some of the spheroid stars from the standard two-component Galaxy model (thin disk plus de Vaucouleurs spheroid) to a third stellar component (a thick disk with a spheroid luminosity function) without disturbing the agreement with observations.

*Subject headings:* galaxies: Milky Way — galaxies: stellar content — galaxies: structure — stars: stellar statistics

## I. INTRODUCTION

The purpose of this paper is to compare the Basel star catalog, constructed over the past 20 yr, with the predictions of the standard Bahcall-Soneira Galaxy model.

The Basel Halo Program on stellar populations and distributions was formulated by Becker as early as 1965 and has been the basis for a large number of observational investigations (Becker 1965, 1967, 1970; Becker and Steppe 1977; Fenkart 1967; 1968, 1969; Fenkart and Wagner 1972, 1975; Schaltenbrand 1974; Fenkart and Schaltenbrand 1977; Yilmaz 1977) and analyses (e.g., Becker 1980; Trefzger 1981; Fenkart 1977, 1980; Buser and Chiu 1981; Spaenhauer, Fenkart, and Becker 1982; Spaenhauer 1982; Buser and Kaeser 1983, 1985; see also Buser 1981). The data are presented in catalogs by Becker and Fenkart (1976); Becker *et al.* (1976); and Becker, Steinlin, and Wiedemann (1978).

The Bahcall-Soneira Galaxy model is based on the assumption that our Galaxy is similar to other galaxies of the same Hubble type. As a first approximation, the two major stellar populations are represented by an exponential disk and a de Vaucouleurs spheroid. The luminosity functions and scale heights are assumed to be constant through the Galaxy and are taken to be the same as are measured for stars near the Sun. In the absence of information to the contrary, it is also assumed that the spheroid stars in the field are similar to stars in globular clusters. This model has been used (Bahcall and Soneira 1980, 1984, hereafter Paper I and Paper II) to predict the observed star colors and number counts in different directions in the Galaxy. The agreement (or disagreement) between the observed and predicted stellar data has been used to delimit the acceptable ranges of parameters (such as density normalizations, scale lengths, and scale heights, see especially Table 1 of Paper II). This procedure is different from the (often unstable) classical method of analysis, which involves inverting the integral equation of stellar statistics. Over the course of the past several years, more detail has been added to the model (the Wielen dip in the disk luminosity function, the ellipticity of the spheroid, and spline fits for the color-magnitude diagrams of the evolved stars) as more detailed observations have been analyzed.

We will use everywhere in this paper the standard parameters of the Galaxy model described in Paper II's discussion of stellar observations in five fields in the Galaxy. Our major finding is that this same Galaxy model permits us to calculate, in good agreement with observations, the colors (in $G-R$) and the apparent magnitudes of stars in the 12 Basel fields analyzed here.

Figure 1 shows the 17 independent fields in which the standard Galaxy model fits well the observed star distributions published by different groups. The existing data are well distributed over the entire Galactic sky outside the region [$|b| < 20°$ or $E(B-V) > 0.1$ mag] in which patchy Galactic obscuration makes comparisons with the model somewhat ambiguous. The shaded area in Figure 1 was not investigated in the present analysis; it has an estimated $E(B-V) > 0.1$ (Burstein and Heiles 1982) or $|b| < 20°$ or both. [In particular, the heavily reddened Basel field near NGC 6171 at $b = 23°$, $l = 3°$ has an estimated $E(B-V) = 0.35$ and was therefore not included in our study.] The Basel observations constitute new tests for the model in 10 different Galactic directions; two directions (SA 57 and SA 51) are in common with directions discussed in Paper II. For two other fields, SA 127 and SA 189, the results are described by Ratnatunga (1983, 1985).

We make many comparisons with observations in this paper. In all these comparisons, the theoretical and the observed distributions refer to the same area of the sky as was covered in the original observations. Thus the ordinates of Figures 4–19 below are stars in the magnitude (or color) interval in the observed area. The total number of stars that were counted or predicted in a given apparent magnitude or color interval can be read directly from the figures.

In § II we summarize briefly the density laws, luminosity functions, and color-magnitude diagrams used in the standard Bahcall-Soneira Galaxy model and show how the $B$ and $V$ colors of the model stars can be transformed to $G$ and $R$. In § III, we review the characteristics of the Basel star catalog. In

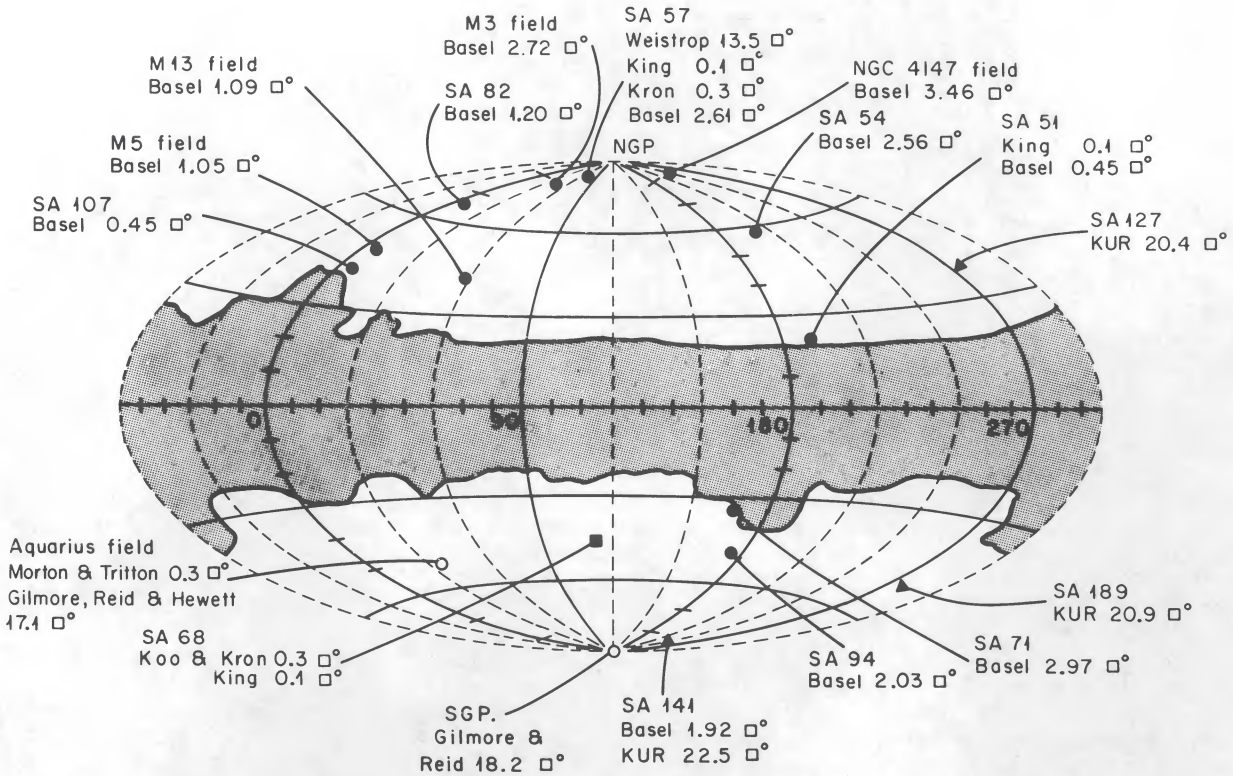


FIG. 1.—Fields in which the Bahcall-Soneira Galaxy model has been tested. The standard Galaxy model (Paper II) fits well the published observations in all of the 17 fields shown. The different observing groups which have studied each field are listed below the label for that field. References to the original observational papers are given in § I of the present paper and in the section discussing each field in Paper II. The zone of avoidance shown by the shaded area has $b < 20°$ or $E(B-V) > 0.1$ mag (according to Burstein and Heiles 1982).

§ IV, we show that the feature which is observed (Da Costa 1982) in globular cluster luminosity functions near $M_V = +1$ to $+4$ is also present in the luminosity function of spheroid field stars. In § V, we compare the model predictions for the color distributions and number counts with the observed distributions in fields in the directions of SA 51, SA 54, SA 57, SA 71, SA 82, SA 94, SA 107, and SA 141, NGC 4147, and M3, M5, and M13. In § VI, we show that the observed star distributions are also consistent with a model suggested by Gilmore, in which the disk and spheroid are essentially the same as in the Bahcall-Soneira model (see Table 3), but which contains a third component—a thick disk with a spheroid luminosity function. The three-component Gilmore model fits the data about as well as the two-component Bahcall-Soneira model. We summarize briefly our principal conclusions in § VII.

## II. THE GALAXY MODEL

### *a) The Ingredients*

The stellar density laws used for the disk and spheroid in our standard model of the Galaxy are given in Table 1; they are the same as in Paper II. We use an exponential disk for the Population I stars and a deVaucouleurs (1959) spheroid for the Population II stars.

The adopted luminosity function of the disk stars is shown in Figure 2*a*. For stars brighter than $M_V = 12.5$, we use the luminosity function determined by Wielen (1974) from observations of nearby stars. We assume for definiteness that the disk luminosity function is constant between absolute visual magnitudes of 12.5 and 16.5 (i.e., down to the end of hydrogen-burning main-sequence stars) and is equal to the observed

TABLE 1

ASSUMED STELLAR DISTRIBUTIONS

| Component | Distribution | Normalization[a] |
|---|---|---|
| Disk..... | $n_D = n_D(R_0) \exp[-z/H(M_V)] \exp[-(x-R_0)/h]$ | $n_D(R_0) = 0.13$ pc$^{-3}$ |
| Spheroid..... | $n_{sph} = n_{sph}(R_0)(R/R_0)^{-7/8}\{\exp[-10.093(R/R_0)^{1/4} + 10.093]\}$[b] | $n_{sph}(R_0) = 0.00026$ pc$^{-3}$ |

NOTE.—Here $z$ is the distance perpendicular to the plane, $x$ is the galactocentric distance in the plane, and $h$ is the disk scale length. Galactocentric distance $R = (x^2 + z^2/\kappa^2)^{1/2}$, where $\kappa$ is the axis ratio and $1-\kappa$ is the ellipticity. We adopt $R_0 = 8$ kpc and $h = 3.5$ kpc. This analytic form of the de Vaucouleurs law is taken from Young 1976. The fraction of disk stars that are on the main sequence is given, in the plane of the disk, by eq. (1) of Bahcall and Soneira 1981 (Paper III).

[a] For $M_V \leq 16.5$ mag.

[b] $R \geq 0.03R_0$.

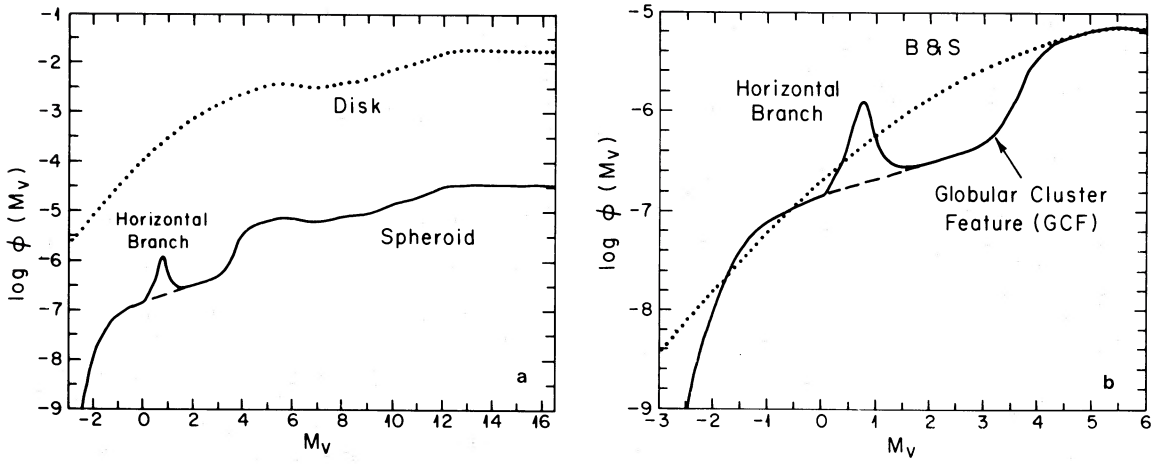


FIG. 2.—(*a*) Adopted disk and spheroid luminosity functions. The luminosity function for the disk is taken from Wielen (1974) for $M_V < 12.5$ and is assumed constant for $M_V > 12.5$. The spheroid luminosity function for $M_V > 4.5$ is assumed for simplicity to have the same shape as that of the disk. It is normalized to contribute 0.2% of the stars in the solar neighborhood. The spheroid luminosity function for $M_V < 4.5$ is assumed to be same as that of the globular cluster 47 Tuc (Da Costa 1982). The two functions were joined smoothly at turnoff $M_V = 4.5$. The contribution from the horizontal branch (peak above the dashed line at $M_V = 0.8$) was assumed to contribute uniformly to the color range $0.6 < B-V < 0.9$. (*b*) The globular cluster feature of the spheroid luminosity function. The spheroid giant branch luminosity function is compared to the monotonic curve used in Paper I. The need for the globular cluster feature is seen mainly from the analysis of star counts of the fainter apparent magnitude range of the Basel fields SA 57 (see Fig. 5) and SA 107 (see Fig. 6).

value at $M_V = 12.5$. (The data considered in this paper do not set useful constraints on the disk luminosity function in the region in which it is assumed flat.) The total number of stars brighter than $M_V = 16.5$ is then 0.13 stars pc$^{-3}$.

There are many determinations in the literature of the local scale heights of disk stars (see references in the legend of Fig. 2 of Paper I). In accordance with this information, we assume that the older main-sequence stars (with $M_V > +5.1$) have an exponential scale height of 325 pc and the younger main-sequence stars (with $M_V < +2.3$) have a scale height of 90 pc. The scale heights are denoted by $H(M_V)$ in Table 1. For $M_V$ between +2.3 and +5.1, the scale height was linearly interpolated between 90 pc and 325 pc (see Fig. 2 of Paper I). We assume that the disk giants have an average scale height of 250 pc and that the white dwarfs have the same scale height as the old stars. The observational constraints on the scale heights are determined in § IX of Paper II.

The scale length of the spheroid that is implied by the density law given in Table 1 was adopted following de Vaucouleurs (1977) and de Vaucouleurs and Buta (1978). We use a value of 8 kpc for the distance of the Sun from the center of the Galaxy. The results we have obtained so far are not sensitive to the precise values of the solar position or the linear scale factors for the spheroid, because the density functions are normalized in the solar neighborhood. The exact shape of the density law is also not well determined. For example, a Hubble density profile can fit the data satisfactorily (see Paper I). On the other hand, the distribution of stars predicted by the model *is* sensitive to the normalization of the spheroid density at the Sun (in stars pc$^{-3}$); we use the normalization determined in Paper II, which differs slightly from that estimated in Paper I and in Bahcall, Schmidt, and Soneira (1983) using a spheroid with an axial ratio of unity. (The spheroid normalization appropriate to the axial ratio of 0.8 used in the present paper is 1/500 the disk density at the Solar position; a value of 1/800 was deduced in Paper I assuming an axial ratio of unity. See also Table 3 of the present paper.) For the relatively bright stars considered here, the predicted color distributions and star counts are also somewhat sensitive to the color-magnitude diagram of the giant branch of the spheroid stars (see Bahcall *et al.* 1983, hereafter Paper IV). Therefore, we consider the effect of different color-magnitude diagrams for the spheroid when we make comparisons with the Basel survey.

The luminosity function for the spheroid that we have adopted as a first approximation is compared in Figure 2*a* with the disk luminosity function and, in Figure 2*b*, with the analytic luminosity function used in the first Bahcall-Soneira Galaxy model. As in Paper II, we have included the Wielen (1974) dip in the spheroid luminosity function (see Fig. 1*a* near $M_V = 7$) as our standard option, since this dip is required to fit the observed color distribution in SA 51 (see Fig. 10 of Paper II).

The feature labeled "globular cluster feature" (GCF) is also included in the standard model discussed here; the GCF was regarded as an option in Paper II because the data discussed in that paper were not sufficient to determine whether this feature is present in the luminosity function of the spheroid field stars (see especially the discussion in Appendix A of Paper II). The need for the GCF is seen from the analysis of the Basel fields SA 57 and SA 107 in § IV of the present paper. The GCF is present in the luminosity functions of all observed globular clusters (see, e.g., Da Costa 1982). Both the old and the new spheroid luminosity functions resemble the measured luminosity functions of globular clusters in the Galaxy within the rather large scatter among the individual functions and are consistent with the Schmidt (1975) data on high-velocity stars (which is sensitive primarily to stars with $+6 < M_V < +12$).

Since the horizontal-branch stars are distributed over a wide color range, their contribution to the spheroid luminosity function was treated separately from the giant branch (see Fig. 2). For the results shown in this paper, the horizontal branch of the field spheroid stars was assumed for definiteness to be centered at $M_V = 0.8$ mag and to contribute uniformly to the color range $0.6 < (B-V) < 0.9$. We have also calculated models using a very different assumed color distribution for the horizontal branch, namely, a Gaussian centered at

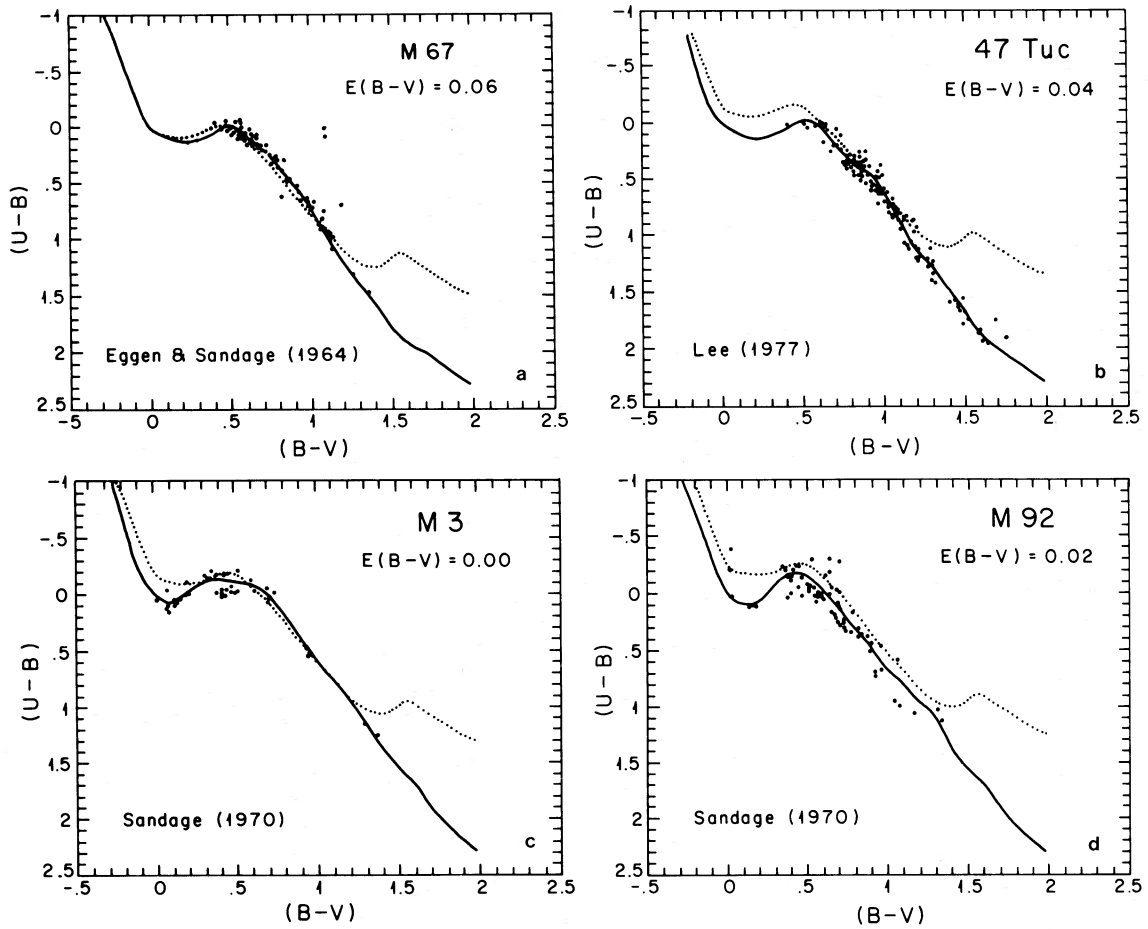


FIG. 3.—Color-color diagrams. The relationships used to estimate $U-B$ from $B-V$. Smooth spline fits through observed data points for giants and dwarfs are used to define independent relations for giants (*solid line*) and dwarfs (*dotted line*). These relations are used to transform the standard galaxy model from $BV$ to $RGU$ system used in the Basel data. (*a*) Observations in M67 used for disk stars. (*b*)–(*d*) Observations in 47 Tuc, M3, and M92 respectively, used for spheroid stars.

$(B-V) = 0.84$ with a FWHM = 0.1 mag. The uniform distribution appears consistent with the available observations of the globular cluster 47 Tuc (see Lee 1977). The Gaussian distribution was tried as an extreme test of the sensitivity of this assumption on the results. The uniform and the Gaussian distributions yield predicted star counts and colors that are similar within the uncertainties of the model and the data.

Over the absolute magnitude range $0 < M_V + 1.6$ mag, corresponding to the horizontal-branch peak the total number of stars is the same to within 10% for the two representations of the luminosity functions shown in Figure 2*b*. The color distributions are also approximately the same.

### *b) Conversion to R, G, and U*

The original version of the Bahcall-Soneira model was formulated so that it could be used to calculate the number of stars with a given absolute visual magnitude and $B-V$ color in each volume element of the Galaxy. In order to analyze the large collection of Basel *RGU* data (see Becker 1946; Buser 1978*a*, *b*), a $U$ color was calculated for each star using the color-color diagrams shown in Figure 3. The transformation to the Basel system was accomplished in the first approximation using the conversion equations published by Steinlin (1968), i.e.,

$$G = V - 0.08(U-B) + 0.93(B-V) \qquad (1a)$$

and

$$(G-R) = 1.15(B-V) - 0.04(U-B) + 0.32\,. \qquad (1b)$$

Since the coefficients of the $U-B$ terms in equations (1) are small, it is not very important which color-color diagram is used to estimate the ultraviolet color. The color-color diagram for M67 (Eggen and Sandage 1964) was used for disk stars (see Fig. 3*a*). For spheroid stars, we used (Figs. 3*b*–3*d*) the color-magnitude diagram and the matching color-color diagram from one of the three globular clusters, 47 Tuc (Lee 1977), M3 (Sandage 1970), or M92 (Sandage 1970). The color-magnitude diagrams we used are shown in Figure 2 of Paper II for 47 Tuc and M92; the M3 diagram was taken from Sandage (1970). For giants the functional dependence of $U-B$ on $B-V$ was defined in terms of a smooth spline fit through the observed $UBV$ photometry, as illustrated in Figure 3. For disk dwarfs the sequence published by Johnson (1966) was used. A constant ultraviolet excess was added to the $U-B$ colors of the disk sequence in order to derive a sequence for spheroid dwarfs; an ultraviolet excess of (cf. Lee 1977; Sandage 1970) 0.1, 0.15, and 0.2 mag was used, respectively, for the diagrams corresponding to 47 Tuc, M3, and M92. The coefficient of $U-B$ in the transformation equation (1) is only 0.08 for $G$ and 0.04 for $G-R$, so the contribution of a typical UV excess to either $G$ or $G-R$ is only of order 0.01 mag. The even smaller

second-order correction due to the variation of UV excess with $B-V$ does not affect any of the comparisons with the data to the accuracy shown.

As stated by Becker and Fenkart (1976), the transformation equations given by equation (1) are inadequate for the reddest stars with $(G-R) > 1.45$. The $G-R$ color given by equation (1) is too small for the very red stars. We therefore stretched linearly the $G-R$ color scale for the red stars, using the FORTRAN statement

```
IF((G − R).gt. 1.45) THEN
    (G − R) = (G − R) + 0.5*((G − R) − 1.45) .   (2)
```

The indicated difference in $G-R$ color could be attributed to a change in $G$ or in $R$ or in both. We have checked by explicit calculation of the color distributions shown later in this paper that, to the accuracy of the existing observations, it is not important how we divide up the color change. In the diagrams shown later, we have assumed that the change in color is caused entirely by a change in $R$, but the corresponding diagrams with all the change attributed to $G$ do not look noticeably different.

The simple stretching given in equation (2) is a first-order approximation to the color transformation predicted by Buser (1984) and Buser and Kaeser (1985) using synthetic colors generated with spectral scans and model atmospheres and was used for all the fields considered in this paper. In order to keep the discussion manageably brief, we refrain from using the more complex theoretical transformations which depend on stellar population and type. We have not analyzed here the $U$ results, because both the data and the color transformations must be known more accurately before this can be done reliably. It will be done in the future by the Basel group.

The reddening is small in all the fields we consider and is estimated from the maps published by Burstein and Heiles (1982). Using a standard option in the export version of the Galaxy model, the observed interstellar extinction and reddening are applied to the intrinsic magnitude and color distributions. We use the following relations:

$$E(B-V) = A(V)/3.00 \tag{3a}$$

and (Steinlin 1968)

$$E(G-R) = A(G)/2.69 = 1.39E(B-V) . \tag{3b}$$

The small amount of reddening that exists in the fields we consider does not significantly affect the calculated color distributions (see the discussion in Paper II of the effect of 0.2 mag visual absorption on the calculated stellar distributions in SA 51, especially Figs. 10*c* and 11*b*–11*d* of Paper II). The individual discussion papers in the Basel series (see references in § I)

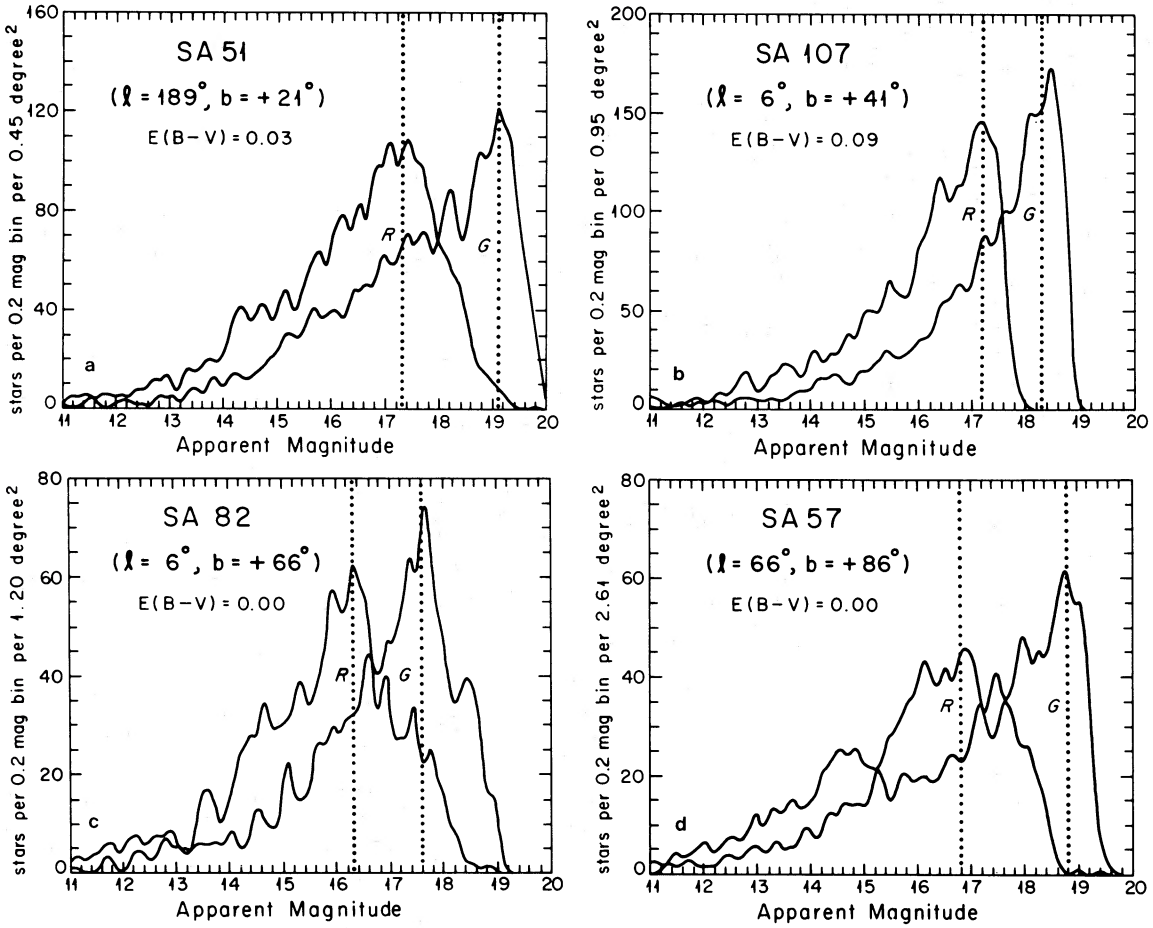


FIG. 4.—Apparent magnitude distributions. Generalized histograms (averaged with a standard deviation $\sigma = 0.08$ mag) of the $R$ and $G$ apparent magnitudes of all the stars in the Basel catalogs of (*a*) SA 51, (*b*) SA 107, (*c*) SA 82, and (*d*) SA 57. The peaks of these distributions were used to select magnitude cutoffs for the analysis of the data. The limits on both $R$ and $G$ that are indicated by the dotted lines were used in both the model and the observed stars included in the analysis.

inferred zero reddening for all 12 fields considered in this paper. The agreement between the observations and the model is essentially the same if the reddening is taken to be exactly zero for all 12 fields, instead of the Burstein-Heiles values.

### III. THE DATA

In order to determine apparent magnitude limits for the analysis, we plotted the number versus magnitude distributions for all stars (excluding the diffuse images classified as N) in the Basel catalog. Illustrative distributions for four of the fields (SA 51, SA 57, SA 82, SA 107) are shown in Figure 4 using the generalized histogram procedure (Searle 1977). Each star is represented in Figure 4 by a Gaussian centered at the measured apparent magnitude with a standard deviation $\sigma$ equal to the measurement uncertainty. We used $\sigma = 0.08$ mag in all the plots in the present paper. The generalized histogram can be regarded as a convolution of the data with a smoothing function that describes the measurement errors.

An apparent magnitude close to the peak of each distribution was selected as a magnitude cutoff. Magnitude limits on both $R$ and $G$ were used to select, before comparison with the model, a well-defined sample in each field. These limits are shown in Figure 4 for the fields illustrated. In all cases, we chose a limiting magnitude for analysis that was close to the peak in the observed apparent magnitude distribution; the observations are incomplete in the region in which the star counts decrease with magnitude.

For each field, we compare in § V the calculated and observed color distributions in three ranges of apparent $G$ magnitudes. The apparent magnitude ranges were selected so that there were approximately equal numbers of stars in the two brightest divisions. The faintest apparent magnitude range was treated separately, since these counts are limited in $R$ as well as $G$. Both limits were imposed on the model and the observations.

The Galactic coordinates and reddening of the 12 Basel fields with $|b| > 20°$ and $E(B-V) < 0.1$ mag are listed in Table 2.

### IV. THE GLOBULAR CLUSTER FEATURE

The GCF in Figure 2 (near $M_V = +1$ to $+4$) is seen clearly in the luminosity function of several globular clusters (Da Costa 1982) and has been advocated by Gilmore as an expected feature of the spheroid field stars (see Gilmore 1984, and references therein). Paper I pointed out that extensive observations in the range $V \approx 16$–18 mag would be required in order to decide if this characteristic feature also appears in the luminosity function of spheroid field stars. We have examined all the fields in the Basel catalog to see which directions and magnitude ranges allow us to test most clearly for the presence

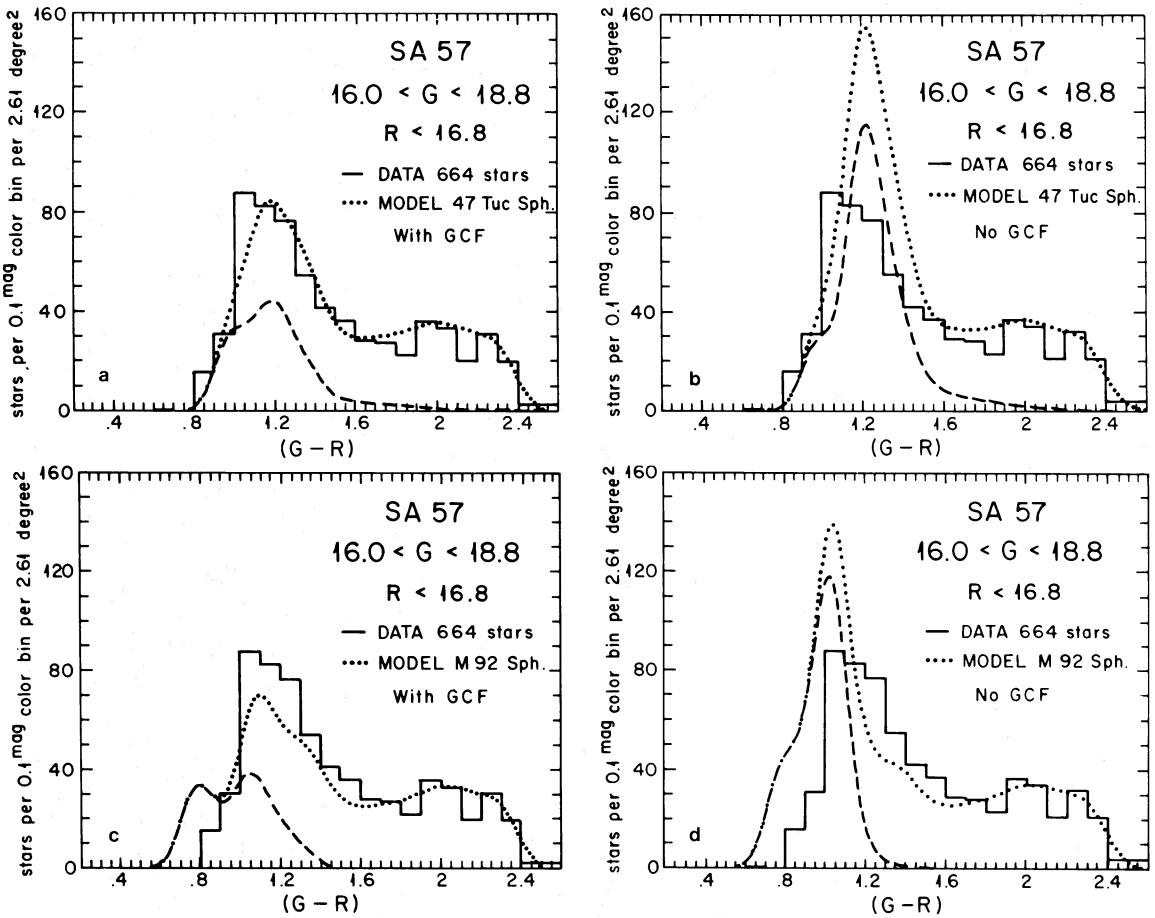


FIG. 5.—The GCF required to fit fainter star counts in SA 57. The observed $G-R$ color distribution (histogram) is compared to the predictions of the model (*dotted line*) for SA 57. The estimated contribution of the spheroid to the counts is shown by the dashed line. (*a*) Color-magnitude diagram of 47 Tuc used for the spheroid. GCF included in the spheroid luminosity function. (*b*) Same, but omitting GCF. (*c*)–(*d*) Same as (*a*) and (*b*), except color-magnitude diagram of M92 used for the spheroid. Reddening $E(B-V = 0.00$ assumed in all the models.

TABLE 2

THE BASEL FIELDS WITH $|b| > 20°$ AND $E(B-V) < 0.1$

| Field | $b$ | $l$ | $E(B-V)$[a] |
|---|---|---|---|
| SA 51 | +21° | 189° | 0.03 |
| SA 54 | +59 | 200 | 0.00 |
| SA 57 | +86 | 66 | 0.00 |
| SA 71 | −34 | 167 | 0.09 |
| SA 82 | +66 | 6 | 0.00 |
| SA 94 | −49 | 175 | 0.06 |
| SA 107 | +41 | 6 | 0.09 |
| SA 141 | −85 | 245 | 0.00 |
| NGC 4147 | +78 | 256 | 0.00 |
| M3 | +78 | 42 | 0.00 |
| M5 | +47 | 4 | 0.02 |
| M13 | +41 | 59 | 0.02 |

[a] From Burstein and Heiles 1982.

of the GCF and have found that the observations of SA 57 (at the North Galactic Pole) and SA 107 ($l = 6°$; $b = +41°$) provide the most sensitive tests.

Figures 5 and 6 show that the GCF is indeed present in the luminosity function of the spheroid field stars. The observed $G-R$ color distributions are compared to the calculated distributions obtained both by including and by omitting the GCF. The solid curve of Figure 2*b* was used to calculate the color histograms that include the GCF, and the smoother (analytic) curve was used for the predictions in Figures 5 and 6 that do not include the GCF.

Figure 5 compares the observed and calculated color distributions for stars in SA 57 that have $G$ magnitudes in the range $16 < G < 18.8$ and $R < 16.8$ mag. The agreement between the observations and the calculated model distributions is good if the GCF is included. On the other hand, if the GCF is omitted, a large peak is predicted near $G-R = 1.2$ mag that is not present in the observations. We have checked that the inferred presence of the GCF in the luminosity function of spheroid field stars is independent of the assumed spheroid color-magnitude diagram. The model calculations shown in Figures 5*a* and 5*b* were obtained using a 47 Tuc (metal-rich) color-magnitude diagram; the results shown in Figures 5*c* and 5*d* were obtained using for illustrative purposes an M92 (metal-poor) color-magnitude diagram. We have made similar calculations using color-magnitude diagrams for the spheroid which are like those of M3 and M13.

Figure 6 shows that the color distributions of stars in SA 107 also require the presence of the GCF.

In all the model calculations discussed in the remainder of this paper, we have included the GCF in the spheroid luminosity function.

## V. COMPARISON OF PREDICTIONS AND OBSERVATIONS: THE 12 BASEL FIELDS

We have compared the observed star counts and color distributions for the 12 Basel fields having $|b| > 20°$ with the results calculated from the Galaxy model. The Galactic coordinates of each of the fields considered here are listed in Table 2.

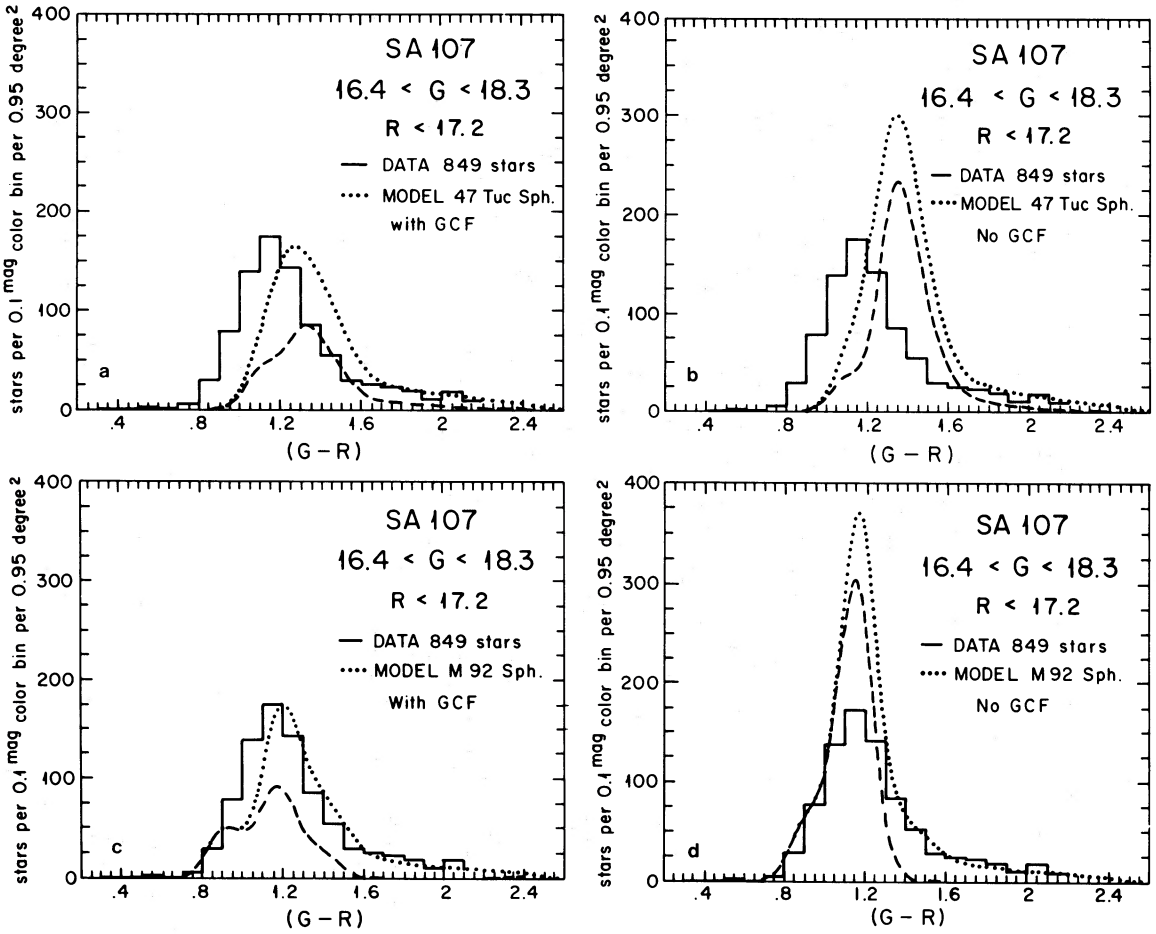


FIG. 6.—The GCF required to fit fainter star counts in SA 107. (*a*)–(*d*) same as in Figs 5*a*–5*d*, except $E(B-V) = 0.09$.

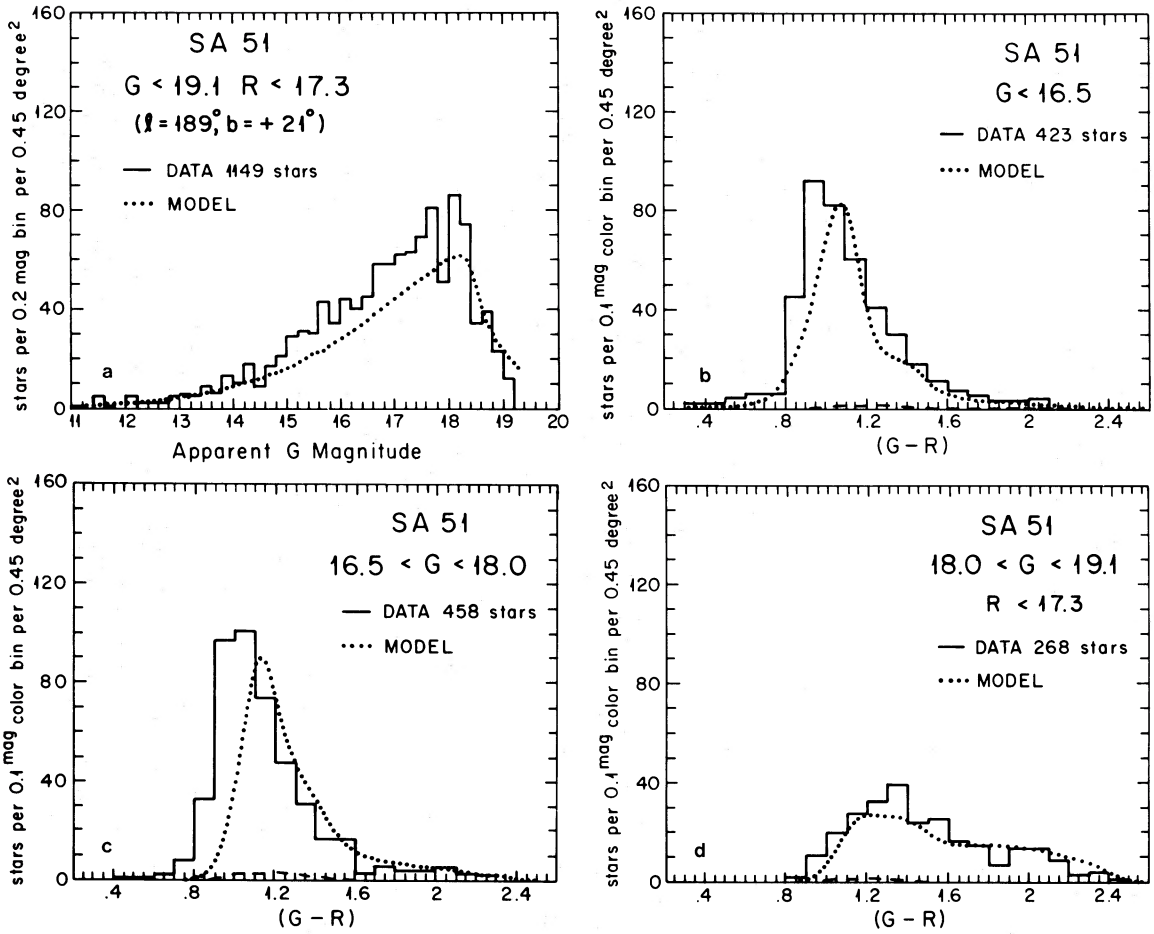


FIG. 7.—Basel *GR* data for field SA 51. (*a*) Compares the apparent distribution in *G* for the total sample selected with both *R* and *G* magnitude limits. The *R* magnitude limit affects only the faintest apparent magnitude range; the two other apparent *G* magnitude ranges were selected to have about equal numbers of stars. (*b*)–(*d*) Compare the observed $G-R$ color distribution (*histogram*) with the distributions calculated from the Bahcall and Soneira Galaxy model (*dotted line*) for three apparent magnitude ranges in SA 51. The contribution of the spheroid to the counts was calculated by assuming a 47 Tuc color-magnitude diagram and is shown by the dashed line. Reddening $E(B-V) = 0.03$ used in the model.

These fields include regions in the direction of the Galactic center and the anticenter, as well as intermediate longitudes. A range of Galactic latitudes is also included, from $|b| = 21°$ to $|b| = 86°$. At Galactic latitudes lower than 20°, the patchy nature of the obscuration in the disk makes comparisons with the model calculations somewhat ambiguous (see Paper I).

The parameters for the Galaxy model are, for all the fields, the same as in Paper II. For definiteness, we have used a color-magnitude diagram for the spheroid field stars that is the same as observed in 47 Tuc (see Fig. 2 of Paper II). We have checked that, with the presently available data, the agreement between the observations and the calculations is not markedly different if an M92 or an M3 color-magnitude diagram is used. The apparent insensitivity of the *G* and *R* data with respect to metallicity—as shown by the present calculations—may not hold for the $U-G$ colors (which will be analyzed in future studies once the calibration and transformation of ultraviolet colors of metal-poor stars is completed, Buser 1984).

Figures 7–18 show the good agreement between the observations and the predictions of the Galaxy model for all 12 of the Basel fields. Each figure compares the calculated model results with the observations of the star counts as a function of apparent magnitude and with the color distributions in each of three magnitude ranges.

## VI. A THICK DISK WITH A SPHEROID LUMINOSITY FUNCTION?

Gilmore and Reid (1983) proposed that the Galaxy has a thick disk with a characteristic scale height that is about 1.5 kpc and which contains approximately 2% of the stars in the solar neighborhood. Gilmore and Reid concluded that the stellar population associated with their proposed thick disk is not the same as the Population II which was defined, for example, by Schmidt (1975), because the local number density of thick disk stars is almost an order of magnitude larger than was estimated for Population II stars by other authors (e.g., Schmidt 1975 and Paper I).

The analysis of Gilmore and Reid (1983) was based on photometric parallaxes, assuming that all the stars were on the main sequence. This assumption was criticized by Bahcall and Soneira (see especially § X of Paper II), who pointed out that most of the spheroid stars in the magnitude range studied by Gilmore and Reid were expected to be giants, not dwarfs, according to the Bahcall and Soneira model. Bahcall and Soneira also pointed out that the blue peak in the faint star counts of Kron (1978, 1980) and of Koo and Kron (1982) could not be explained by a thick disk but instead required the presence of a spheroidal component.

The parameters of a thick disk must be chosen carefully in

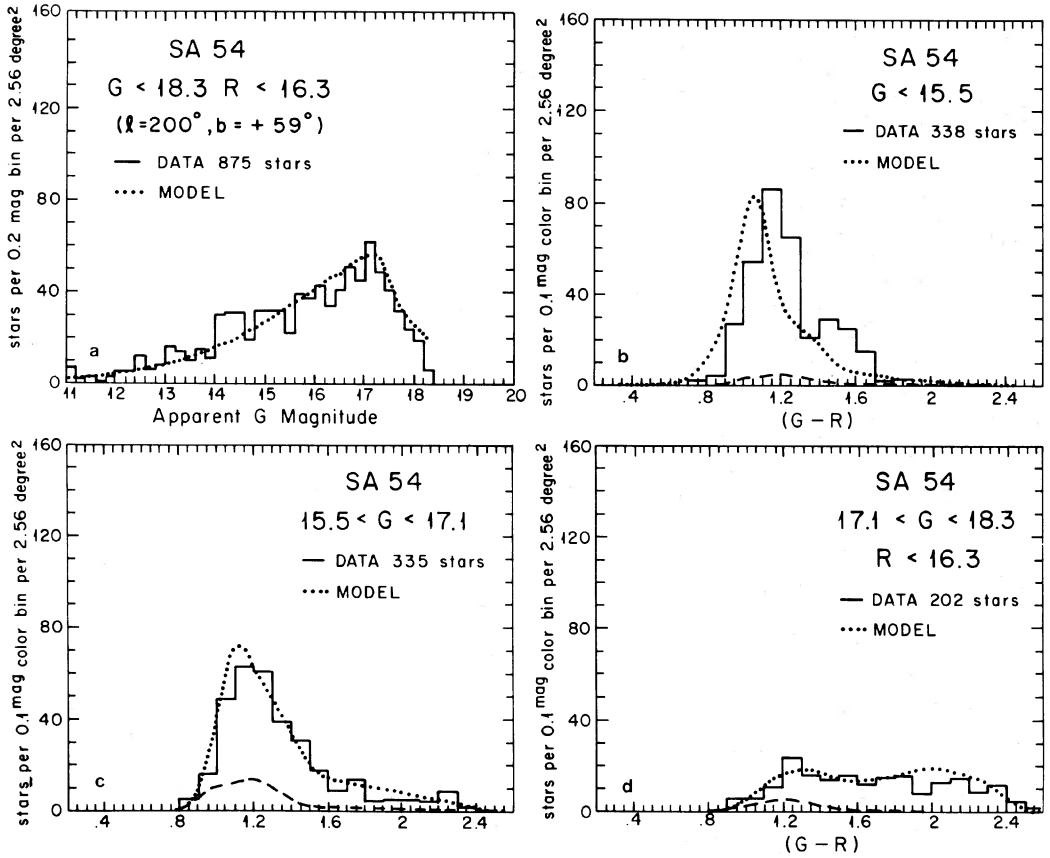


FIG. 8.—Basel *GR* data for field SA 54. As in Fig. 7, except that $E(B-V) = 0.00$.

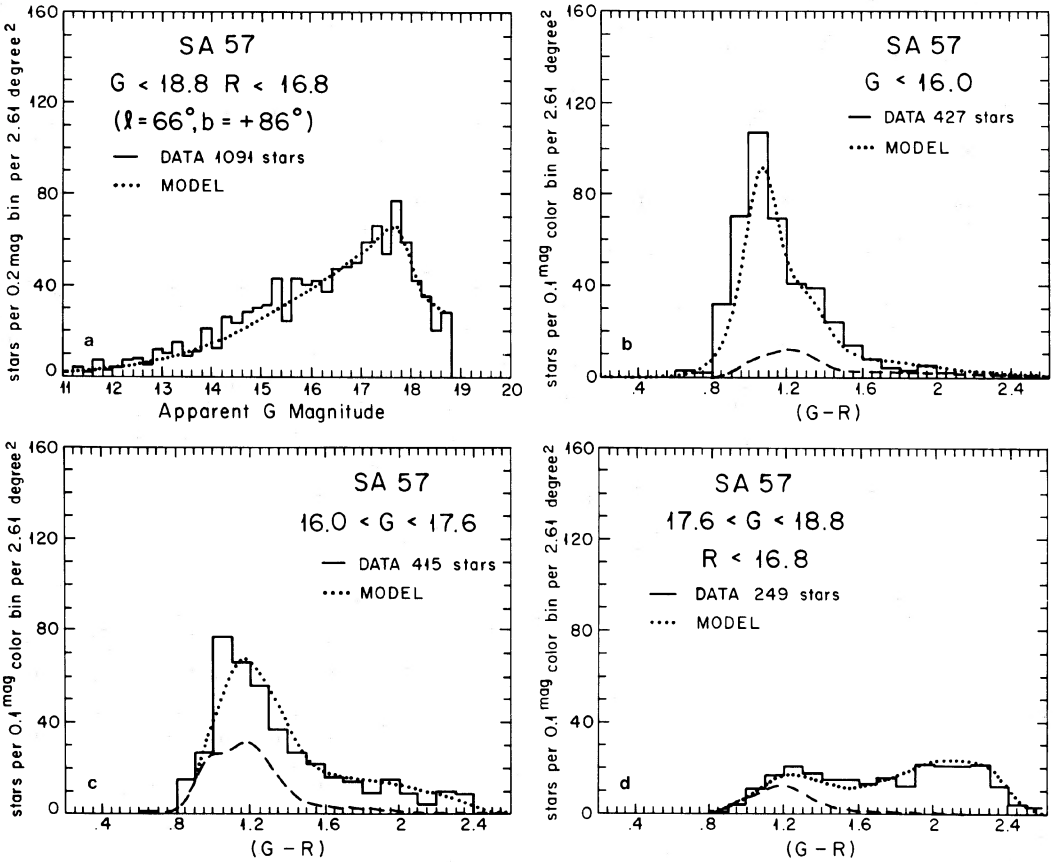


FIG. 9.—Basel *GR* data for field SA 57. As in Fig. 7, except that $E(B-V) = 0.00$.

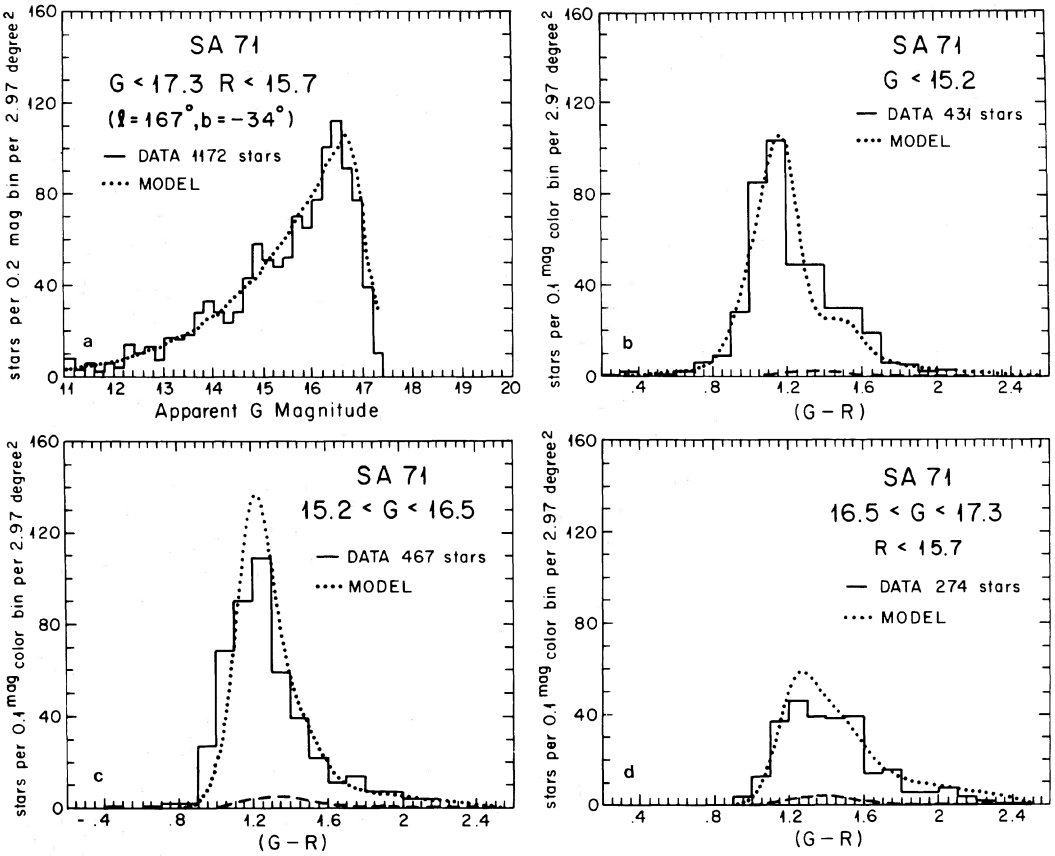


FIG. 10.—Basel *GR* data for field SA 71. As in Fig. 7, except that $E(B-V) = 0.09$.

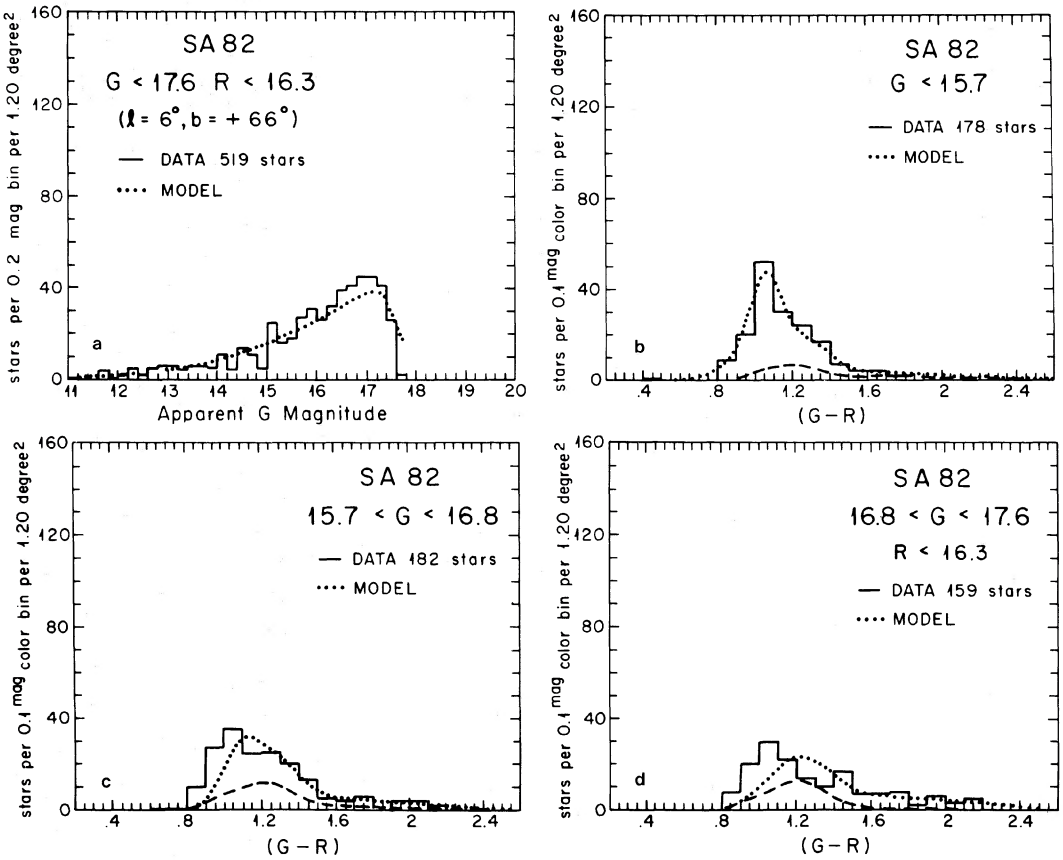


FIG. 11.—Basel *GR* data for field SA 82. As in Fig. 7, except that $E(B-V) = 0.00$.

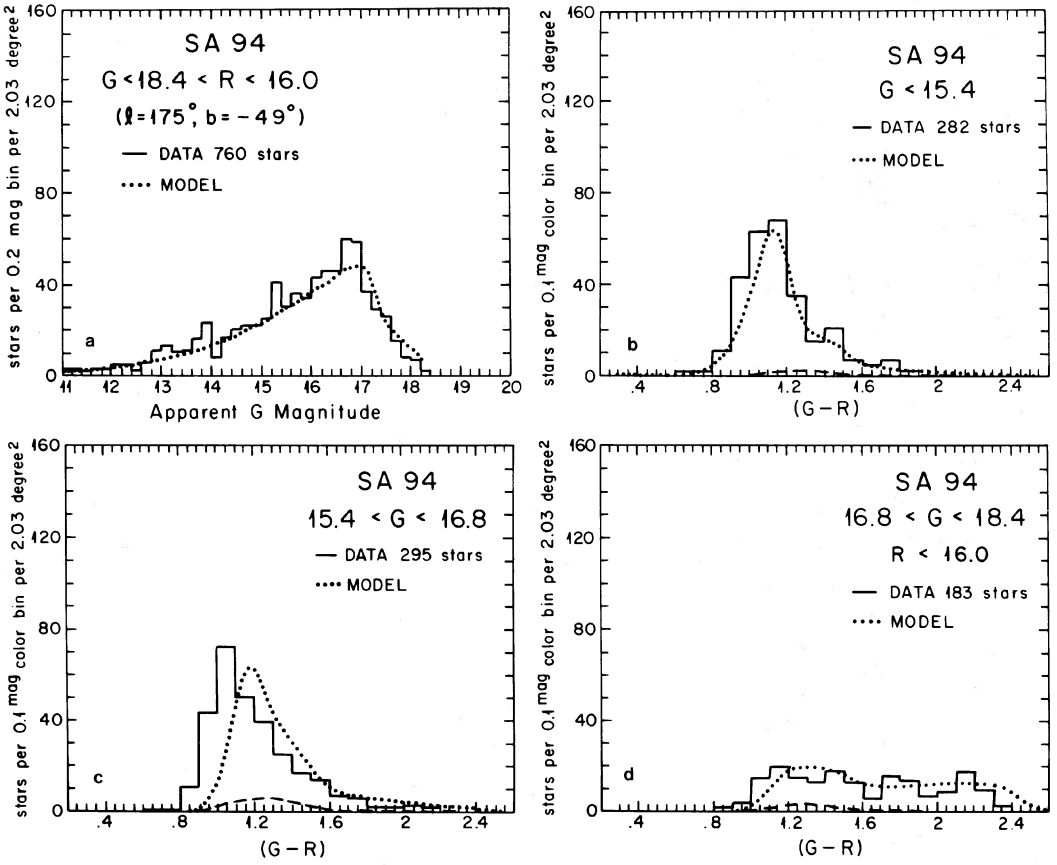


FIG. 12.—Basel *GR* data for field SA 94. As in Fig. 7, except that $E(B-V) = 0.06$.

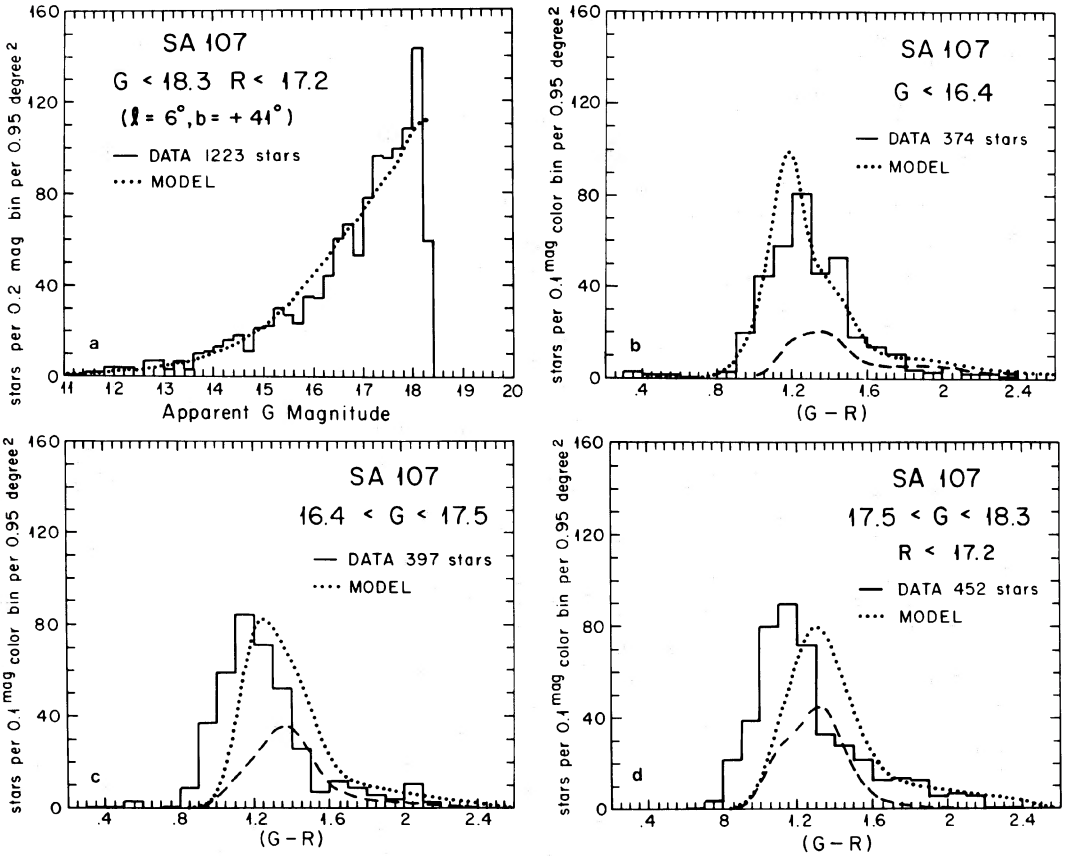


FIG. 13.—Basel *GR* data for field SA 107. As in Fig. 7, except that $E(B-V) = 0.09$.

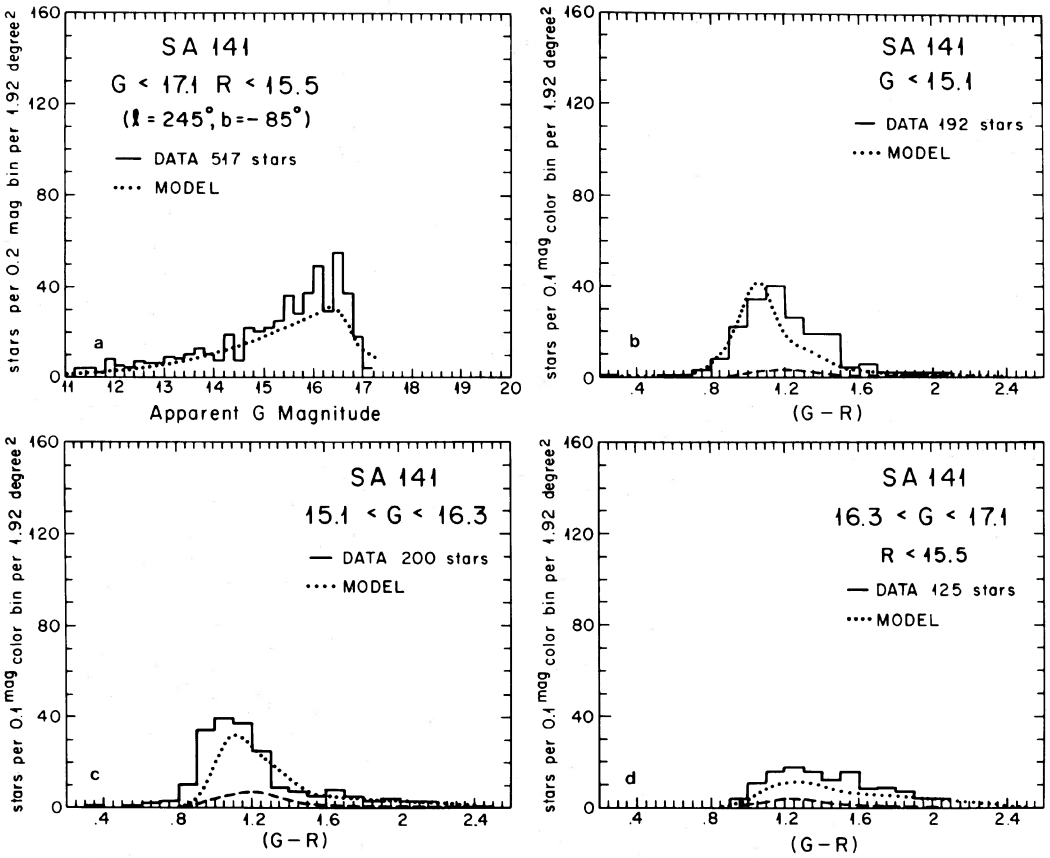


FIG. 14.—Basel *GR* data for field SA 141. As in Fig. 7, except that $E(B-V) = 0.00$.

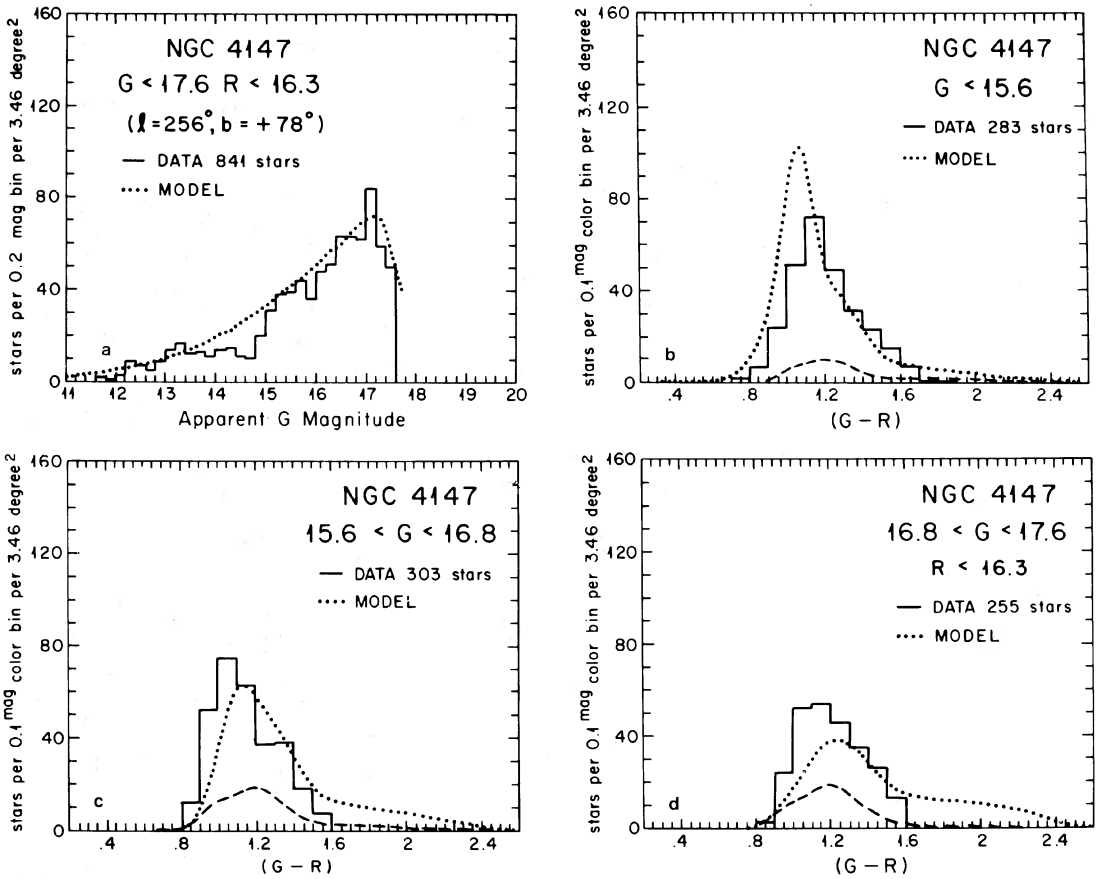


FIG. 15.—Basel *GR* data for field near NGC 4147. As in Fig. 7, except that $E(B-V) = 0.00$.

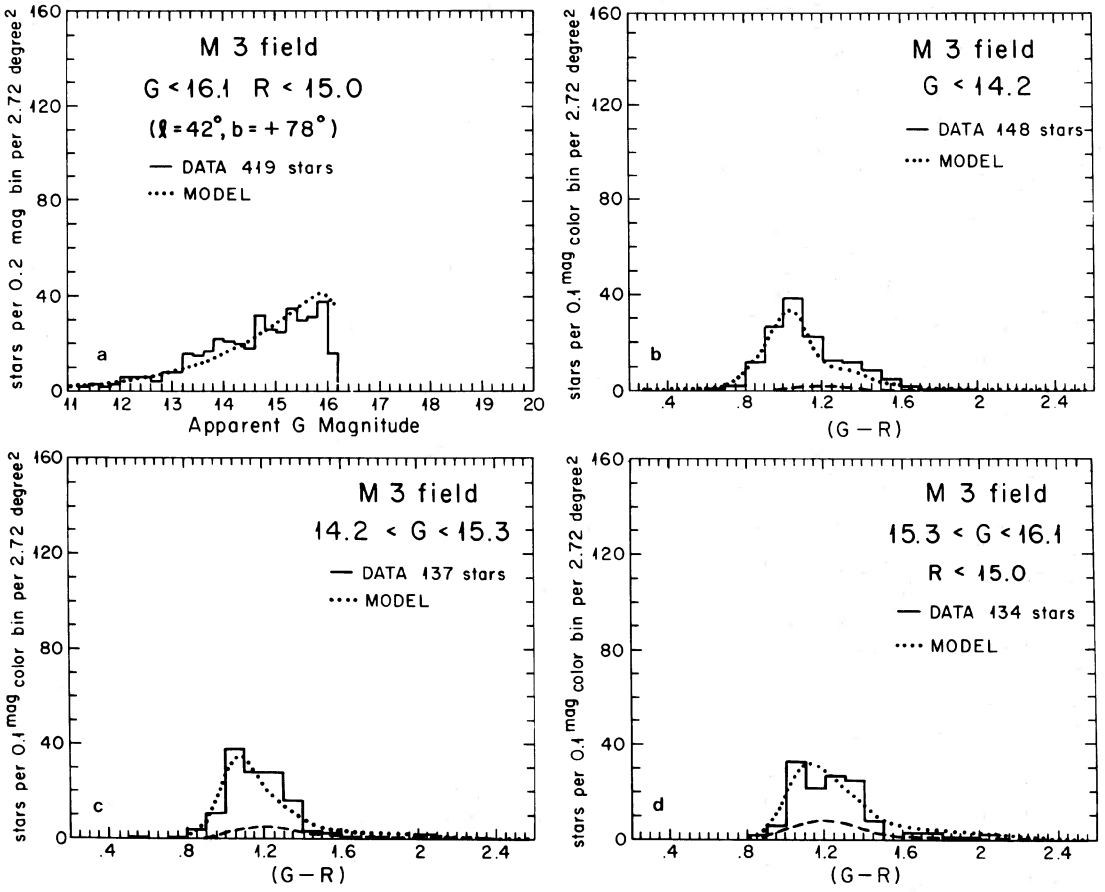


FIG. 16.—Basel *GR* data for field near M3. As in Fig. 7, except that $E(B-V) = 0.00$.

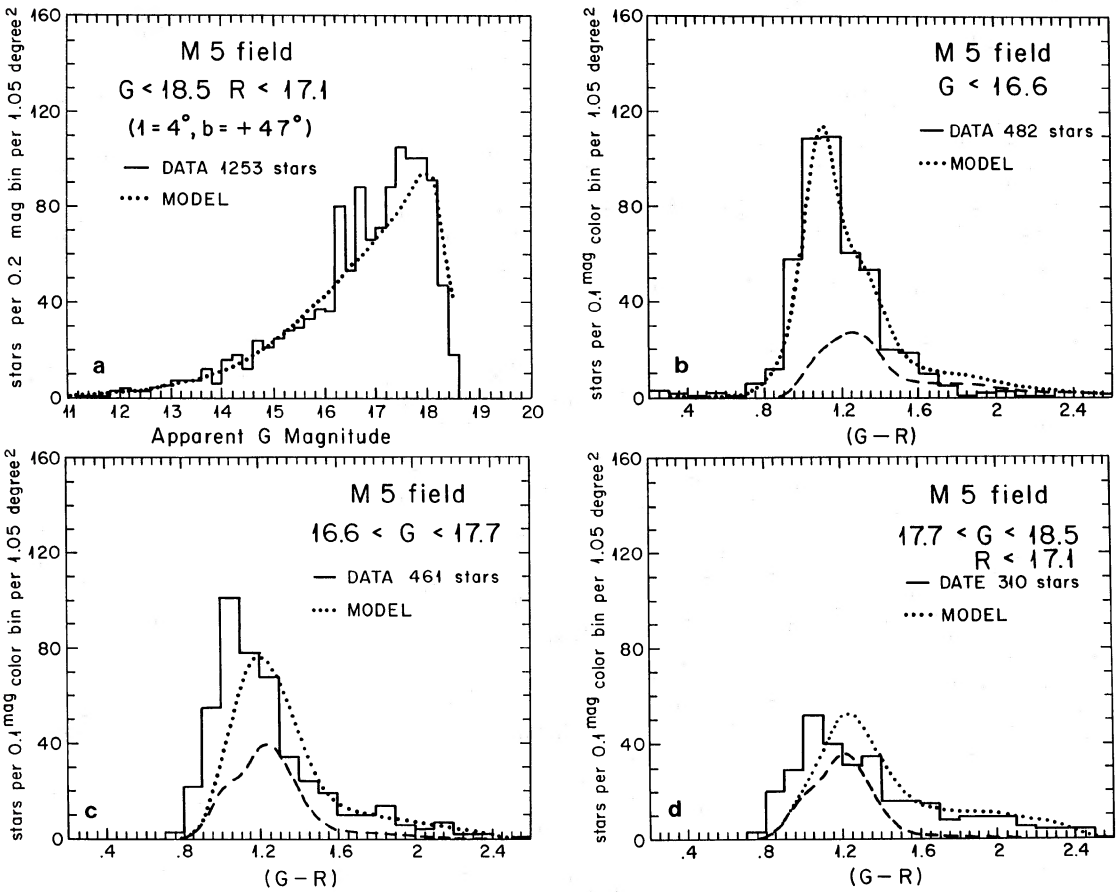


FIG. 17.—Basel *GR* data for field near M5. As in Fig. 7, except that $E(B-V) = 0.02$.

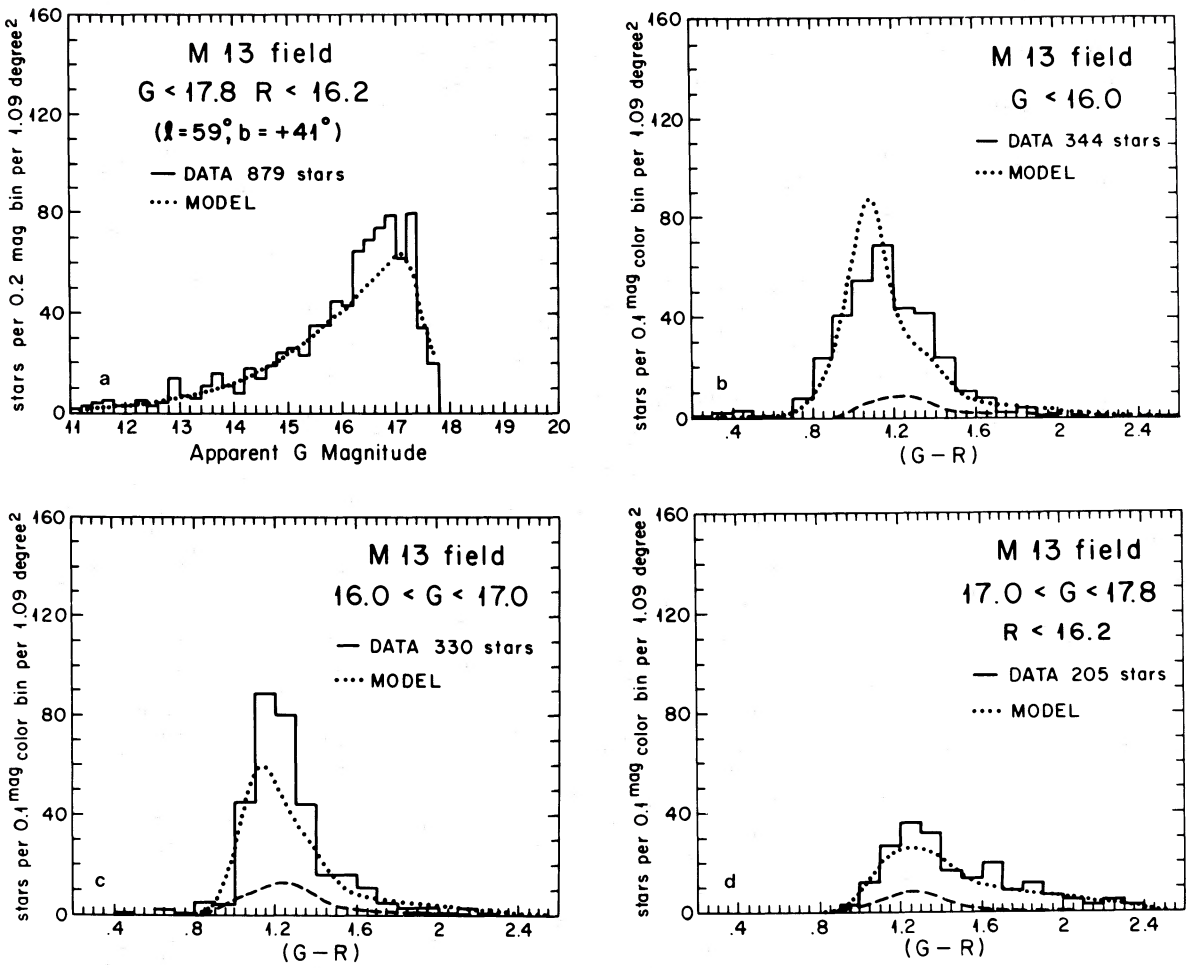


FIG. 18.—Basel *GR* data for field near M13. As in Fig. 7, except that $E(B-V) = 0.02$.

order to avoid filling up the valley at $B-V \approx +1$ between the two peaks, due to the thin disk and the spheroid, in faint star counts (see Fig. 7 and Table 5 of Bahcall, Schmidt, and Soneira 1983). The Gilmore and Reid (1983) parameters (1.45 kpc, 2% normalization) are in conflict with observation if a disk luminosity function is assumed for the thick disk (see Fig. 17 of Paper II).

Gilmore (1984) has discussed a model in which the thin disk and spheroid are essentially the same as in the Paper I model, but which also contains a third component. This extra component is a thick disk with a *spheroid luminosity function*, having about 10% of the mass of the thin disk and an order of magnitude more Population II stars than in the spheroid. The parameters of this model are listed in Table 3, where it is compared with the Bahcall and Soneira model (Paper I and Paper II). Table 3 makes it clear that the Gilmore model must yield essentially the same results as the Bahcall-Soneira model, since the differences in parameter choices are minor.

In order to verify quantitatively the similarity of the two models, we recomputed, using the parameters of Gilmore (1984), the predicted star distributions for all the fields considered in this paper and in Paper II. Following Gilmore (1984), we have assumed the *same* luminosity function, shown in Gilmore's Figure 6, for both the thick disk and the spheroid. This luminosity function is similar to the spheroid luminosity function adopted in the present paper (see Fig. 2); the differences between Gilmore's function and ours are less than the differences that exist between the reported luminosity functions of individual globular clusters.

Figures 19*a*–19*d* shows the satisfactory agreement between the Gilmore model and the Basel observations for four illustrative fields, SA 51, SA 57, SA 82, and SA 107. Figures 19*e*–19*f* show the agreement between the model and the observed (Kron 1980) color distributions for the fainter stars in SA 57 and SA 68.

Given the assumption by Gilmore (1984) that the thick disk has a spheroid luminosity function, the thick disk contribution is not separable from the Bahcall-Soneira spheroid in any of the 17 fields or colors we have considered.

## VII. SUMMARY AND DISCUSSION

The main result of this paper is that the standard Galaxy model of Paper II predicts star counts and color distributions that are in good agreement with the observations in 12 Basel fields, listed in Table 2, spread throughout the Galaxy. Altogether, this model accounts well for the observations in 17 different fields, shown in Figure 1, over a large range in apparent magnitudes and in several color bands (see also Paper I and Paper II). A quick perusal of the 48 panels in Figures 7–18 shows the generality of the model; these panels cover the color distributions and number counts in the different directions and magnitude ranges of the Basel survey. The color histograms

have different shapes in the various fields, but all the shapes are satisfactorily described by the same model.

The comparison with observations in SA 57 and SA 107 provides new information about the field spheroid stars; namely, the GCF shown in Figure 2 is present in the luminosity function of field stars. The evidence for this conclusion is described in § II and is illustrated in Figures 5 and 6. This result provides a partial answer to the question posed by Kraft (1983): "Are the spheroid field stars the same as globular cluster stars?" The two populations are similar in that they both exhibit a GCF in their luminosity functions. However, the two populations also differ in that the blue tip of the horizontal branch is missing in the spheroid field stars (see Table 5 of Paper II, and Paper IV).

The good agreement between the calculated and observed stellar distributions shows that the normalizations for the

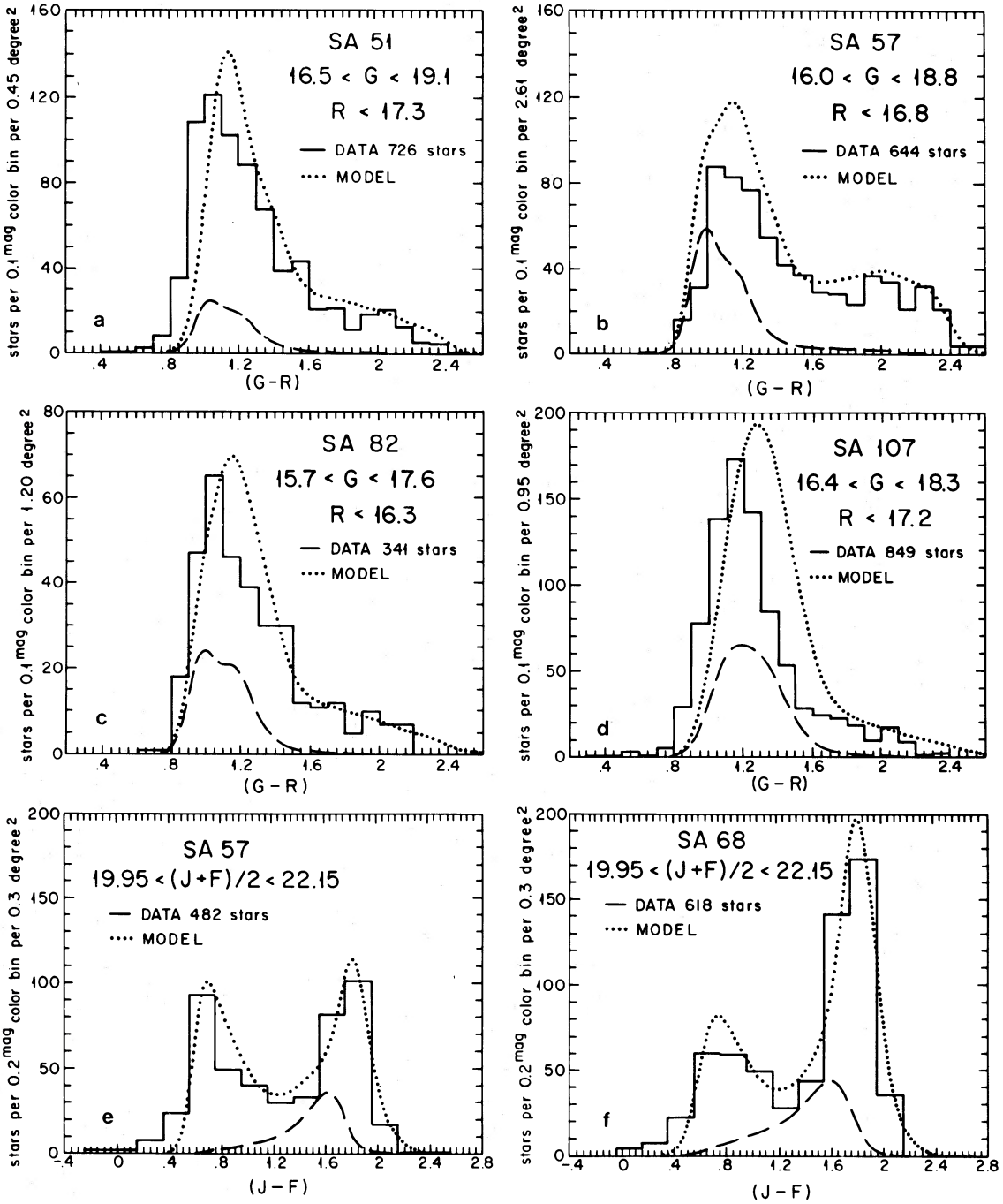


FIG. 19.—Possible contribution of a thick disk. (*a*)–(*d*) Compare the observed $G-R$ color distribution (*histogram*) to that estimated by a composite model (*dotted line*) which includes a thick disk with a spheroid luminosity function and the most recent parameters assumed by Gilmore (1984, see Table 3 of this paper). The parameters for two of the components, the thin disk and normal spheroid are essentially those of Paper I. Figs. 19*a*–19*d* illustrate the results respectively for SA 51, SA 57, SA 82, and SA 107 using $E(B-V) = 0.03, 0.00, 0.00$, and 0.09 respectively. The calculated contributions of Gilmore's thick disk to the counts is shown by the dashed line. (*e*)–(*f*) The $(J-F)$ distribution from this same model for the fainter star counts published by Kron (1980) for SA 57 and SA 68. The thick disk of Gilmore is not separable from the normal spheroid in any of the fields or colors that we have considered.

TABLE 3

COMPARISON OF MODEL PARAMETERS: BAHCALL-SONEIRA AND GILMORE

| Parameter | Paper I | Paper II | Gilmore 1984 |
|---|---|---|---|
| Solar galactocentric distance (kpc) | 8 | 8 | 9 |
| *Disk*: | | | |
| Scale length (kpc) | $3.5 \pm 0.5$ | 3.5 | 4.0 |
| Scale height (old stars) (pc) | 325 | 325 | 325 |
| Disk luminosity functions | Wielen (no dip) | Wielen (dip) | Wielen (dip) |
| Color-magnitude diagram | M67 | M67 | Chiu 1980 |
| *Spheroid*: | | | |
| Local normalization (to disk) | 0.00125 | 0.002 | 0.00125 |
| Density law | de Vaucouleurs (also Hubble) | de Vaucouleurs | de Vaucouleurs |
| Minor/major axis | 0.85 | $0.80^{+0.20}_{-0.05}$ | 0.85 |
| Effective radius (kpc) | 2.7 | 2.7 | 3.0 |
| Luminosity function | Analytic | Globular cluster | Gilmore 1984, Fig. 6 |
| *Thick disk*: | | | |
| Local normalization | ... | ... | 0.02 |
| Exponential scale height (kpc) | ... | ... | 1.3 |
| Exponential scale length (kpc) | ... | ... | 4.0 |
| Luminosity function | ... | ... | Gilmore 1984, Fig. 6 |
| Color-magnitude diagram | ... | ... | 47 Tuc |

density laws given in Table 1 are correct to an accuracy of about 25% for all the directions and magnitude ranges we have investigated (all the fields shown in Fig. 1). The acceptable ranges of other model parameters are given in Table 1 of Paper II.

At least two major stellar components are required by the observations (see Papers I and II): (1) a Population I thin disk (implied, e.g., by the red peak in color histograms like Fig. 8 of Paper I or Fig. 5 of Paper II); and (2) an approximately round ($b/a \approx 0.8$) Population II spheroid (implied by the blue peaks in the same color histograms of Papers I and II). These are the two major stellar components that are described in the original Bahcall-Soneira Galaxy model (Paper I). In addition, it is possible to add other stellar components without destroying the agreement with observations, provided they do not dominate the predicted star distributions in any of the 17 fields shown in Figure 1. For example, it will be necessary in future infrared studies at low Galactic latitudes of the Galactic central region to add a separate stellar component to describe the concentration represented by the nuclear component in the mass model of Bahcall, Schmidt, and Soneira (1983) (for a description of this component see Oort 1965). As an example of allowed relatively small changes in the model, we find, in agreement with the suggestion of Gilmore (1984), that the observations are consistent with the existence of a thick disk which has a spheroid luminosity function and 10% of the mass of the thin disk. However, the available observations do not *require* the existence of this thick disk. The parameters advocated by Gilmore (1984), which are listed in Table 3, are within the estimated uncertainties in the standard Galaxy model. The predictions made with Gilmore's three-component model are indistinguishable, within the existing observational uncertainties, from the distributions predicted by the standard two-component model for all 17 of the fields that we have examined.

Since the standard Galaxy model fits all the available data, the model is useful as a guide in planning new observations. For projects in which the background or foreground density of certain types of stars is important, the model code can be run to see how many stars of a given color (type) it predicts in any specified direction and apparent magnitude range. Moreover, the model can be used to delimit the allowed range of Galactic parameters (see Papers I and II, especially Table 1 of Paper II) and as a tool in suggesting the most appropriate ways to reveal new Galactic characteristics or populations.

This work was supported by the National Science Foundation grants PHY-8217352 and NAS8-32902, and by the Swiss National Science Foundation.

REFERENCES

Bahcall, J. N., Schmidt, M., and Soneira, R. M. 1983, *Ap. J.*, **265**, 730.
Bahcall, J. N., and Soneira, R. M. 1980, *Ap. J. Suppl.*, **44**, 73 (Paper I).
———. 1981, *Ap. J.*, **246**, 122 (Paper III).
———. 1984, *Ap. J. Suppl.*, **55**, 67 (Paper II).
Bahcall, J. N., Soneira, R. M., Morton, D. C., and Tritton, K. P. 1983, *Ap. J.*, **272**, 627 (Paper IV).
Becker, W. 1946, *Veröff. Sternw. Göttingen*, **79**.
———. 1965, *Zs. Ap.*, **62**, 54.
———. 1967, *Zs. Ap.*, **66**, 404.
———. 1970, *Astr. Ap.*, **9**, 204.
———. 1980, *Astr. Ap.*, **87**, 80.
Becker, W., and Fenkart, R. 1976, *Photometric Catalogue for Stars in Selected Areas and other Fields in the RGU-System*, Vol. **1** (Basel: Astr. Inst. Univ. Basel).
Becker, W., Fenkart, R., Schaltenbrand, R., Wagner, R., and Yilmaz, F. 1976, *Photometric Catalogue for Stars in Selected Areas and other Fields in the RGU-System*, Vol. **2** (Basel: Astr. Inst. Univ. Basel).
Becker, W., Steinlin, U., and Wiedemann, D. 1978, *Photometric Catalogue for Stars in Selected Areas and other Fields in the RGU-System*, Vol. **5** (Basel: Astr. Inst. Univ. Basel).
Becker, W., and Steppe. H. 1977, *Astr. Ap. Suppl.*, **28**, 377.
Burstein, D., and Heiles, C. 1982, *A.J.*, **87**, 1165.
Buser, R. 1978*a*, *Astr. Ap.*, **62**, 411.
———. 1978*b*, *Astron. Astrophys.*, **62**, 425.
———. 1981, ed., *Galaktische Struktur und Entwicklung* (Basel: Astr. Inst. Univ. Basel).
———. 1984, in preparation.
Buser, R., and Chiu, L. T. G. 1981, *Mitt. Astr. Gesellschaft*, **52**, 40.
Buser, R. and Kaeser, U. 1983, in *IAU Colloquium 76, The Nearby Stars and the Stellar Luminosity Function*, ed. A. G. D. Philip and A. R. Upgren (Schenectady: Davis), p. 147.
———. 1985, *Astr. Ap.*, **145**, 1.
Chiu, L.-T. G. 1980, *Ap. J. Suppl.*, **44**, 31.
Da Costa, G. S. 1982., **87**, 990.
de Vaucouleurs, G. 1959, *Handbuch der Physik*, **53**, 311.
———. 1977, *A.J.*, **82**, 456.
de Vaucouleurs, G., and Buta, R. J. 1978, *A.J.*, **83**, 1383.
Eggen, O. J., and Sandage, A. R. 1964, *Ap. J.*, **140**, 130.
Fenkart, R. P. 1967, *Zs. Ap.*, **66**, 390.
———. 1968, *Zs. Ap.*, **68**, 87.

Fenkart, R. P. 1969, *Astr. Ap.*, **3**, 228.
———. 1977, *Astr. Ap.*, **56**, 91.
———. 1980, *Astr. Ap.*, **91**, 352.
Fenkart, R. P., and Schaltenbrand, R. 1977, *Astr. Ap. Suppl.*, **27**, 409.
Fenkart, R. P., and Wagner, R. 1972, *Astr. Ap.*, **19**, 1.
———. 1975, *Astr. Ap.*, **41**, 315.
Gilmore, G. 1984, *M.N.R.A.S.*, **207**, 223.
Gilmore, G., and Reid, N. 1983, *M.N.R.A.S.*, **202**, 1025.
Gilmore, G., Reid, N., and Hewitt, P. 1985, *M.N.R.A.S.*, **213**, 257
Johnson, H. L. 1966. *Ann. Rev. Astr. Ap.*, **4**, 193.
Koo, D. C., and Kron, R. G. 1982, *Astr. Ap.*, **105**, 107.
Kraft, R. P. 1983, *Highlights Astr.* **6**, 129.
Kron, R. G. 1978, Ph.D. thesis, University of California, Berkeley.
———. 1980, *Ap. J. Suppl.*, **43**, 305.
Lee, S. W. 1977, *Astr. Ap. Suppl.*, **27**, 381.
Morton, D. C., and Tritton, K. P. 1982, *M.N.R.A.S.*, **198**, 669.
Oort, J. H. 1965, in *Stars and Stellar Systems, Galactic Structure*, ed. A. Blaauw and M. Schmidt (Chicago: University of Chicago Press), p. 455.
Ratnatunga, K. U. 1983, Ph.D. thesis, Australian National University, Canberra.
———. 1985, in preparation.
Reid, G., and Gilmore, G. 1982, *M.N.R.A.S.*, **201**, 73.
Sandage, A. 1970, *Ap. J.*, **162**, 841.
Schaltenbrand, R. 1974, *Astr. Ap. Suppl.*, **18**, **18**, 27.
Schmidt, M. 1975, *Ap. J.*, **202**, 22.
Searle, L. T. 1977, in *The Evolution of Galaxies and Stellar Populations*, ed. B. M. Tinsley and R. B. Larson (New Haven: Yale Univ. Obs.), p. 219.
Spaenhauer, A. 1982, *Bull. Inf. Centre Donnée Stellaire*, **22**, 12.
Spaenhauer, A., Fenkart, R. P., and Becker, W. 1982, *Mitt. Astr. Gesellschaft*, **57**, 316.
Steinlin, U. W. 1968, *Zs. Ap.*, **69**, 276.
Trefzger, Ch. F. 1981, *Astr. Ap.*, **95**, 184.
Wielen, R. 1974, *Highlights Astr.* **3**, 395.
Yilmaz, F. 1977 *Pub. Istanbul Obs.*, No. 98.
Young, D. J. 1976, *A.J.*, **81**, 807.

JOHN N. BAHCALL and KAVAN U. RATNATUNGA: Institute for Advanced Study, Princeton, NJ 08540

ROLAND BUSER, R. P. FENKART, and ANDREAS SPAENHAUER: Astronomisches Institut der Universität Basel, CH-4102, Binningen/BL, Switzerland